

5 Extensions of the Cylindrical Model

by Lutz Jaitner, August through October, 2018

The cylindrical model, as defined by simplifications (3) through (21), was build to be simple, rather than precise. Accordingly, some terms are missing in the Hamiltonian.

The following extensions of the cylindrical model are attempting to explore some of these missing terms, which had been “approximated away” in the first instance. The extensions themselves are also approximations.

5.1 Polarization of the Electron Gas Around the Nuclei

Simplification (7) models the nuclear charges a uniform jellium, rather than charged points in space. The resulting electron orbitals are therefore not forming density cusps around the nuclei as one would expect to occur in reality.

It is intuitively clear, that the resulting binding energy with the jellium approach is higher (i.e. more endothermic) than in reality, where the electrons in the cusps on average come closer to the positive charge of the nuclei.

As an extension of the cylindrical model one can quantify the static electron polarization around the nuclei (i.e. cusps) by means of Thomas-Fermi screening. The contribution of the cusps to the total binding energy of a CP can be estimated with this.

Assuming the electron temperature in a CP is $T_e < 10^5 K$ and the Fermi energy of the electrons (i.e. the difference between the highest and the lowest occupied electron eigenvalue) is $\bar{E}_F > 10^4 eV$, then $k_B T_e < 8.6 eV \ll \bar{E}_F$.

Therefore, Thomas-Fermi can be applied to a CP safely at the $T_e \rightarrow 0$ limit.

For a Fermi gas at $T = 0$ the state density at the Fermi edge is:

$$(169) \quad \frac{\partial n}{\partial \mu} = \frac{3}{2} \frac{n}{\bar{E}_F}, \text{ where } n \text{ is the electron number density and } \mu \text{ is the chemical potential}$$

Usually, the above equation is used for computing the screening wave number of Thomas-Fermi screening. However, the electron gas of a CP is not free, because it is bound to a potential well in radial direction. As can be seen in Figure 19, the electron state density distribution in a CP differs from a free electron gas.

The figure shows the state density distribution of a typical CP configuration. The Fermi energy in this case is 166 keV, the maximum electron number density is $n=0.38 \text{ 1/pm}^3$ and the maximum state density per electron is 11.4 MeV^{-1}

With these values the maximum state density computes as:

$$(170) \quad \max\left(\frac{\partial n}{\partial \mu}\right) = 1.9 \frac{\max(n)}{\bar{E}_F} = \frac{1.9}{e} \frac{\max(-\bar{\sigma}_e)}{\bar{E}_F},$$

where $n = -\bar{\sigma}_e/e$ is the electron number density according to (42)

For computing the Thomas-Fermi screening length in the region of highest electron density, equation (170) will be used below, rather than equation (169).

However, there are uncertainties, which could hamper the application of Thomas-Fermi screening to CP:

- A strong magnetic field is present, with unclear (at least to the author) consequences to the polarization of the electrons
- It may be incorrect to assume full 3-D screening, because CP mostly extend in axial direction and have a small radius (in the order of 25 pm, depending on configuration)

Additionally, the Fermi wave number k_F is not a well-defined quantity in CP, because:

- The axial wave numbers at the occupation edge (Fermi level) are covering the hole range of k-values (in Figure 17), i.e. from 24.9 pm^{-1} through 28.0 pm^{-1} . The mean of these values is 26.4 pm^{-1} , which is translating into an axial De Broglie wave length of 0.237 pm .
- The axial wave numbers are greatly inflated/shifted by the magnetic field. Without this shift, the wave axial numbers at the Fermi level would probably be an order of magnitude smaller

- The maximum occupied wave number is greatly anisotropic in CP. In radial direction the shortest De Broglie wave length is 2.46 pm, which translates to a wave number of 4.92 pm^{-1}

The Thomas-Fermi model is valid only for wave numbers much smaller than the Fermi wave number k_F . In other words: Modeling the polarization cusps at distances to the nucleus shorter than 2 pm is probably of little value, because the Thomas-Fermi model is just not accurate in this range.

Despite all these uncertainties and in lack of a good alternative, the Thomas-Fermi theory will be applied in the following.

With linearized Thomas-Fermi screening the induced electron charge density is approximated by:

$$(171) \quad \bar{\sigma}_e^{\text{induced}}(\vec{r}_n) \approx -e^2 \max\left(\frac{\partial n}{\partial \mu}\right) \Phi^{\text{screened}}(\vec{r}_n) \approx 1.9e \frac{\bar{\sigma}_e^\infty}{\bar{E}_F} \Phi^{\text{screened}}(\vec{r}_n),$$

where Φ^{screened} shall be the screened potential of a nucleus and \vec{r}_n is the position relative to the nucleus

In the above equation Φ^{screened} is defined to approach zero at large \vec{r}_n . $\bar{\sigma}_e^\infty$ is the maximum value of the electron charge density at large \vec{r}_n .

Relation (171) can be converted into a wave-number-dependent dielectric function (i.e. the relative permittivity):

$$(172) \quad \varepsilon_r(k) = 1 + \frac{k_s^2}{k^2}, \text{ where } k \text{ is the wave number of the polarization (in momentum space)}$$

$$\text{and } k_s = \sqrt{\frac{e^2 \max\left(\frac{\partial n}{\partial \mu}\right)}{\varepsilon_0}} = \sqrt{-\frac{1.9e \bar{\sigma}_e^\infty}{\varepsilon_0 \bar{E}_F}} \text{ (in SI units) is the Thomas-Fermi screening wave number}$$

The dielectric function can be used to compute the effects of polarization in momentum space:

$$(173) \quad \varepsilon_r(k) = \frac{\bar{\sigma}^{\text{extern}}(k)}{\bar{\sigma}^{\text{extern}} + \bar{\sigma}_e^{\text{induced}}(k)} = 1 - \frac{\bar{\sigma}_e^{\text{induced}}(k)}{\bar{\sigma}^{\text{extern}} + \bar{\sigma}_e^{\text{induced}}(k)} = \frac{\Phi^{\text{extern}}(k)}{\Phi^{\text{extern}}(k) + \Phi_e^{\text{induced}}(k)}, \text{ where}$$

$\bar{\sigma}_e^{\text{induced}}(k)$ and $\Phi_e^{\text{induced}}(k)$ are the electron charge density and the potential caused by polarization.
 $\bar{\sigma}^{\text{extern}}(k)$ and $\Phi^{\text{extern}}(k)$ are the charge density and the potential, which caused the polarization.

The Poisson's equation relates the electric potential with the volume charge density:

$$(174) \quad \nabla^2 \Phi(\vec{r}) = -\frac{\bar{\sigma}(\vec{r})}{\varepsilon_0}, \text{ where } \vec{r} \text{ is the position}$$

A nucleus with a point charge of $Q_n = eZ$ will produce a Thomas-Fermi-screened potential of:

$$(175) \quad \Phi^{\text{screened}}(k) = \frac{e}{\varepsilon_0} \frac{Z}{k^2 + k_s^2}$$

The above equation Fourier-transforms to:

$$(176) \quad \Phi^{\text{screened}}(\vec{r}_n) = \frac{e}{4\pi\varepsilon_0} \frac{Z}{r_n} \exp(-k_s r_n), \text{ where } \vec{r}_n \text{ is the position relative to the nucleus}$$

The quantity $1/k_s$ is the Thomas-Fermi screening length. With the values of $\bar{E}_F = 166 \text{ keV}$ and $\bar{\sigma}_e^\infty = 0.38e \cdot \text{pm}^{-3}$ the screening length computes as:

$$(177) \quad \frac{1}{k_s} = \sqrt{-\frac{\varepsilon_0 \bar{E}_F}{1.9e \bar{\sigma}_e^\infty}} = 3.57 \text{ pm}$$

The screening length is bit shorter than the minimum distance between the nuclei (4.32 pm for the same configuration). This might help to understand, why in a CP the nuclei can have such high density.

Using (176) with (177), the screened potential is plotting as following:

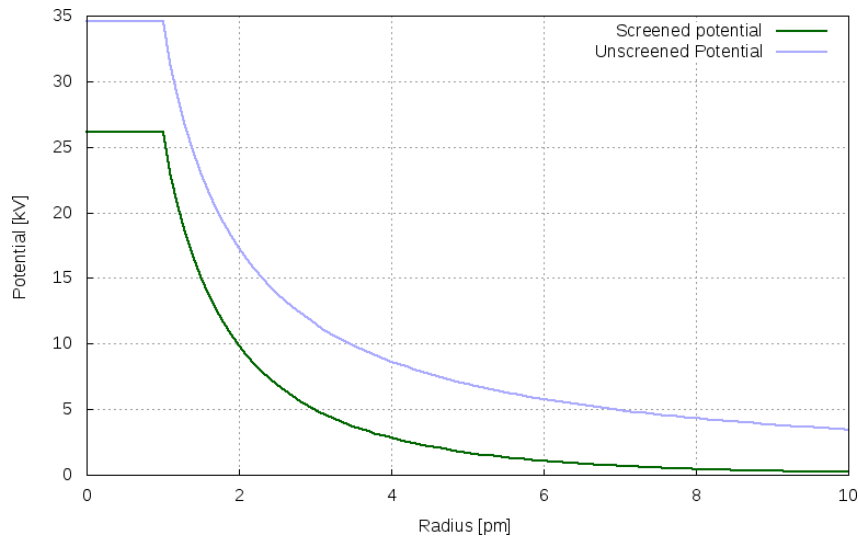


Figure 8 Screened and unscreened potential of a nucleus with nuclear charge $Z=24$. The diverging values have been cropped at Radius < 1 pm

The difference between the unscreened potential and the screened potential is not varying much with the radius. This difference can hence be characterized by a constant, i.e. the screening potential:

$$(178) \quad \Phi_s = \frac{eZk_s}{4\pi\epsilon_0} = 9.7kV, \text{ with } Z = 24 \text{ and } k_s^{-1} = 3.57 \text{ pm}$$

In line with the above example, for the fusion of hydrogen ($Z=1$) with chromium ($Z=24$) the screening potential energy would be $U_s = 9.7keV$. For d-d fusion there would be $U_s = 404eV$ and the minimum distance between neighboring deuterons would be 1.50 pm.

The induced electron density according to equation (171) is plotting as following:

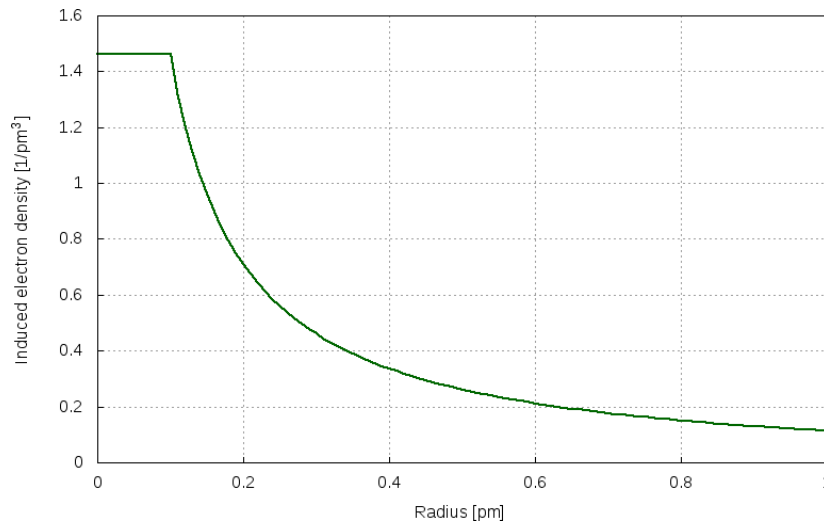


Figure 9 Induced electron density around the nucleus of Figure 8. The diverging values have been cropped at Radius < 0.1 pm

How much induced charge will be accumulated in a sphere around a nucleus (cusp) with a radius of one third of the distance to the nearest neighbor nucleus (1.44 pm)? This question can be answered by integrating equation (171) and using (176):

$$\begin{aligned}
 (179) \quad Q_e^{cusp} &\approx 1.9e \cdot 4\pi \frac{\bar{\sigma}_e^\infty}{E_F} \int_0^{1.44 \text{ pm}} \Phi^{screened}(\vec{r}_n) r_n^2 dr_n \\
 &= 1.9 \frac{e^2 Z}{\epsilon_0} \frac{\bar{\sigma}_e^\infty}{E_F} \int_0^{1.44 \text{ pm}} r_n \exp(-k_s r_n) dr_n \\
 &= -1.9 \frac{e^2 Z}{\epsilon_0} \frac{\bar{\sigma}_e^\infty}{E_F k_s} \left[r_n \exp(-k_s r_n) + \frac{1}{k_s} \exp(-k_s r_n) \right]_0^{1.44 \text{ pm}} = -1.50e
 \end{aligned}$$

The induced charge in the cusps is less than two electrons for a nucleus with $Z=24$. This can arguably be interpreted to mean, that **even the innermost electron shell (K-shell) is delocalized**. This interpretation would be supporting the basic assumption of the cylindrical model, that all electrons of a CP are delocalized.

The electron density $\bar{\sigma}_e^{induced}/e$ surpasses $\bar{\sigma}_e^\infty/e = 0.38/pm^3$ (i.e. the electron density at large \vec{r}_n) only at $r_n < 0.355 \text{ pm}$. For the purpose of estimating the binding energy contribution of the cusp, the integral can therefore be limited to $r_n < 0.355 \text{ pm}$.

The binding energy between a nucleus ($Z=24$) and the charge induced by this nucleus in the cusp is:

$$\begin{aligned}
 (180) \quad U_{cusp} &= 4\pi \int_0^{0.355 \text{ pm}} \bar{\sigma}_e^{induced}(\vec{r}_n) \Phi^{unscreened}(\vec{r}_n) r_n^2 dr_n = 4\pi \cdot 1.9e \frac{\bar{\sigma}_e^\infty}{E_F} \int_0^{0.355 \text{ pm}} \Phi^{screened}(\vec{r}_n) \Phi^{unscreened}(\vec{r}_n) r_n^2 dr_n \\
 &= 4\pi \cdot 1.9e \frac{\bar{\sigma}_e^\infty}{E_F} \left(\frac{eZ}{4\pi\epsilon_0} \right)^2 \int_0^{0.355 \text{ pm}} \exp(-k_s r_n) dr_n \\
 &= 4\pi \cdot 1.9e \frac{\bar{\sigma}_e^\infty}{E_F} \left(\frac{eZ}{4\pi\epsilon_0} \right)^2 \frac{1}{k_s} [-\exp(-k_s r_n)]_0^{0.355 \text{ pm}} = -22.1 \text{ keV}
 \end{aligned}$$

Dividing the result of equation (180) by the number of electrons per nucleus ($=26.4$) yields an **estimated contribution of the cusp to the binding energy per electron of -0.837 keV**.

Given, that the contribution of the cusps is so small and there are so many uncertainties in applying Thomas-Fermi screening to CP, the author decided to not include the cusp contribution in the Hamiltonian during the simulation runs.

5.2 Exchange-Correlation Energy Functionals

Local-density approximations (LDA) are approximations to the exchange-correlation energy functional in density functional theory (DFT) that depend solely upon the value of the electronic density at each point in space (and not, for example, derivatives of the density).

Using LDA for a CP (in units of the Hartree energy, cylindrical coordinates) provides:

$$(181) \quad E_{xc}[\sigma_e] = \frac{2\pi L}{\lambda_n} \int_0^\infty |\sigma_e(r)| \mathcal{E}_{xc}[\sigma_e] r dr,$$

where σ_e is the electron charge density in natural units according to (112), L is the axial length of the CP in units of the Bohr radius, r is the relative radius coordinate according to (111) and \mathcal{E}_{xc} is the exchange-correlation energy per particle of a homogeneous electron gas of charge density σ_e .

The exchange-correlation energy is decomposed into exchange and correlation terms linearly,

$$(182) \quad \mathcal{E}_{xc} = \mathcal{E}_x + \mathcal{E}_c$$

However, the DFT formalism breaks down, to various degrees, in the presence of a magnetic field. In such a situation, the one-to-one mapping between the ground-state electron density and wave function is lost. Generalizations to include the effects of magnetic fields have led to the current density functional theory and magnetic field density functional theory. For reasons of simplicity, these theories are not engaged here.

The approximation quality of DFT/LDA achievable by neglecting the magnetic field is therefore seen as merely “experimental”. Nonetheless, such rogue approach is detailed below.

The analytically known exchange energy functional in LDA is (in units of the Hartree energy, cylindrical coordinates):

$$(183) \quad \varepsilon_x[\sigma_e] = -\frac{3}{4} \sqrt{\frac{3}{\pi}} |\sigma_e(r)|$$

The Chachiyo correlation energy functional (in units of the Hartree energy), which is based on many-body perturbation theory, is applicable to the full range of densities:

$$(184) \quad \varepsilon_c[\sigma_e] = \frac{\ln(2)-1}{2\pi^2} \ln\left(1 + \frac{b}{r_s} + \frac{b}{r_s^2}\right),$$

$$\text{where } r_s = \sqrt[3]{\frac{3}{4\pi} \frac{1}{|\sigma_e|}} \text{ is the Wigner-Seitz parameter and } b = 20.4562557$$

The Wigner-Seitz parameter r_s is defined as the radius of a sphere which encompasses exactly one electron, divided by the Bohr radius.

With the CP configuration of chapter 6.1 the exchange energy per electron is -658 eV and the correlation energy per electron is -4.6 eV. These values are so small (compared to the other terms of the Hamiltonian), that they were not included in the simulation runs. Also, the values could be incorrect due to the strong magnetic field.